ISSN 007-2621

No. 3 — 1986

published quarterly

Technical Review

To Advance Techniques in Acoustical, Electrical and Mechanical Measurement

Deconvolution for Modal Decoupling

Oblique DOF

Brüel & Kjær

PREVIOUSLY ISSUED NUMBERS OF BRÜEL & KJÆR TECHNICAL REVIEW

2-1986 Quality in Spectral Match of Photometric Transducers
Guide to Lighting of Urban areas
1-1986 Environmental Noise Measurements
4-1985 Validity of Intensity Measurements in Partially Diffuse Sound Field
Influence of Tripods and Microphone Clips on the Frequency Response of Microphones
3-1985 The Modulation Transfer Function in Room Acoustics
RASTI: A tool for evaluating auditoria
2-1985 Heat Stress
A New Thermal Anemometer Probe for Indoor Air Velocity Measurements
1-1985 Local Thermal Discomfort
4-1984 Methods for the Calculation of Contrast
Proper Use of Weighting Functions for Impact Testing
Computer Data Acquisition from B&K Digital Frequency Analyzers 2131 / 2134 using their Memory as a Buffer
3-1984 The Hilbert Transform
Microphone System for Extremely Low Sound Levels
Averaging Times of Level Recorder 2317
2-1984 Dual Channel FFT Analysis (Part II)
1-1984 Dual Channel FFT Analysis (Part I)
4-1983 Sound Level Meters – The Atlantic Divide
Design principles for Integrating Sound Level Meters
3-1983 Fourier Analysis of Surface Roughness
2-1983 System Analysis and Time Delay Spectrometry (Part II)
1-1983 System Analysis and Time Delay Spectrometry (Part I)
4-1982 Sound Intensity (Part II Instrumentation and Applications)
Flutter Compensation of Tape Recorded Signals for Narrow Band Analysis
3-1982 Sound Intensity (Part I Theory).
2-1982 Thermal Comfort.
1-1982 Human Body Vibration Exposure and its Measurement.
4-1981 Low Frequency Calibration of Acoustical Measurement Systems. Calibration and Standards. Vibration and Shock Measurements.
3-1981 Cepstrum Analysis.
2-1981 Acoustic Emission Source Location in Theory and in Practice.
1-1981 The Fundamentals of Industrial Balancing Machines and their Applications.

(Continued on cover page 3)

TECHNICAL REVIEW

No. 3 — 1986

Contents

A METHOD OF DETERMINING THE MODAL FREQUENCIES OF STRUCTURES WITH COUPLED MODES*

by

Ole Døssing

ABSTRACT

The problem of modal coupling encountered in vibration response, leads to obscurity of the discrete nature of the system's dynamic properties. The coupling effect can be significantly reduced by deconvolution, which is obtained by weighting the response signal from an impact excitation or a measured impulse response. The transform of the weighted function is called the mode spectrum, the properties of which will be discussed, indicating some guidelines for practical application.

The theory of deconvolution will be described together with experimental results from analytical data and from measurements made on a real structure with coupled modes.

SOMMAIRE

Les problèmes soulevés par le couplage modal, et que l'on rencontre dans des réponses de vibrations, tendent à obscurcir la nature discrète des propriétés dynamiques des systèmes. L'effet de couplage peut être réduit de façon significative par déconvolution, obtenue par pondération du signal de réponse à une excitation par impact, ou une réponse impulsionnelle mesurée. La transformée de la fonction pondérée est appelée le spectre de mode, dont les propriétés seront discutées, et dont on donnera les principes directeurs pour des applications pratiques.

La théorie de la déconvolution sera décrite en même temps que des résultats expérimentaux à partir de données d'analyse et de mesures prises sur une structure réelle possédant des modes couplés.

ZUSAMMENFASSUNG

Modale Kopplung in der Schwingcharakteristik verschleiert die diskrete Natur der dynamischen Eigenschaften des Systems. Durch Deconvulution (Ent-Faltung) läßt

* First published in IMAC IV, 1986

sich der Kopplungseffekt signifikant vermindern. Sie läßt sich durch Bewertung des Antwortsignals einer Stoßerregung oder einer gemessenen Impulserregung ermitteln. Die Transformation der bewerteten Funktion wird als „Mode"-Spektrum bezeichnet. Die Eigenschaften dieser Funktion werden diskutiert und Richtlinien für die praktische Anwendung gegeben.
Neben der Theorie der Deconvolution werden experimentelle Ergebnisse von analytischen Daten und von Messungen an einem realen System mit gekoppelten Schwingungsformen gegeben.

Introduction

Although a mode is an independent property of a linear structure, interaction between modes may result in a coupled response. The coupling makes it difficult to identify the modes in a measurement, which in turn complicates the parameter estimation procedure. For instance, if some modes are overlooked due to modal coupling, the resulting model may be too poor for subsequent simulations.

The free vibration of a single degree of freedom system following an excitation with an impulse, can be regarded as a sinusoidal oscillation at the damped natural frequency multiplied, or weighted, by an exponential decay function. The spectrum can be viewed as a sine spectrum convolved with the transform of the exponential function. For systems with multiple degrees of freedom this convolution leads to smearing and modal coupling.

The coupling effect can be significantly reduced by deconvolution of a measured frequency response. The deconvolution is obtained by weighting the response signal from an impact excitation or a measured impulse response. The transform of the weighted function is called the *mode spectrum* and is a line spectrum where each line represents a damped natural frequency.

This paper presents the theory of the deconvolution together with experimental results from analytical data and from measurements made on a real structure with coupled modes. The properties of the mode spectrum based on weighting parameters are discussed, indicating some guidelines for practical application.

The experiments show that an efficient decoupling is achieved in the mode spectrum, particularly when the coupling is caused by large

variations in the mode strength. A peak sharpening effect, observed as a reduction of the peak bandwidth for highly damped modes, also results from the deconvolution.

A complete dynamic description of a structure can generally be achieved via a discrete set of *modes* of vibration.

Modal Coupling

Although each mode is an independent property of a structure, a vibration response may show strong interaction between modes or, as it is often called, *modal coupling*. This obscures the discrete nature of the system's dynamic properties.

In terms of the linear independancy (orthogonality) of modes, the phrase "modal coupling" seems a little misleading, but due to the traditional use of these words, we shall continue with this terminology in the following.

In experimental modal analysis we often describe the dynamic properties of systems in the frequency domain, using frequency response measurements. The degree of modal coupling in a frequency response measurement depends on the ratio between the frequency spacing, the damping, and the strength difference of the neighbouring modes. In other words the heavier the modes are damped, the greater the difference in strength, or the less the modes are spaced, the more coupled is the response.

Extreme coupling occurs when the modal frequency is identical for two or more modes, and separation is not possible using monoreference techniques [1]. Moderate coupling is observed with modes of the same strength whose frequency spacing is of the same size as the bandwidth of the modes.

When the strength of neighbouring modes is different – which is generally the case for mechanical systems where magnitude variations over 50 dB are seen – weak modes can be totally obscured by even distant but strong modes.

Further, modes with high damping spread their influence over wide frequency bandwidths, hiding both themselves and neighbouring modes.

Fig. 1 shows an analytically generated frequency response containing modes that are coupled due to the above causes.

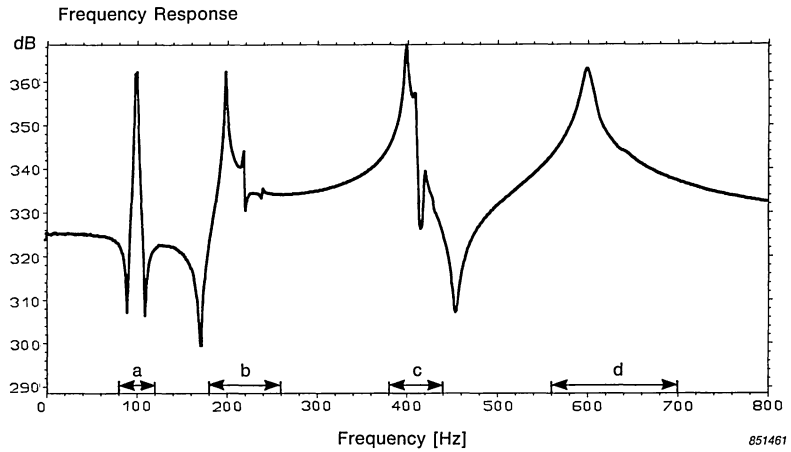

Fig. 1. Frequency response with high modal coupling
Range a: two modes with very close modal frequencies
b: three modes covering a 40 dB dynamic range in strength
c: four modes with 52 dB dynamic range and close modal frequencies
d: three modes, highly damped, close modal frequencies and 40 dB dynamic range

The effect of Modal Coupling

When modes couple, it is difficult to determine the number of modes in a frequency response measurement, and this in turn creates problems when the optimum curve fitting model and technique are to be chosen [2].

For example, if one overlooks the fact that a peak contained more than one mode, and applies a single DOF technique, the estimated modal parameters will be totally erroneous. If modes are omitted from the model, giving a truncated model, subsequent simulations are poor.

Weak modes concealed between strong modes may also be overlooked, again resulting in truncated models.

When the existence of several modes in a particular frequency band is realized, and a multiple DOF model is chosen for the parameter estimation, the number of expected modes often has to be given – or alterna-

tively the computational modes must subsequently be edited from the data.

In other words, it would be a great advantage to have a technique or tool to determine the number of modes and their frequencies in a measurement.

In the following text we shall analyze the phenomena that lead to modal coupling, and based on this analysis suggest a method for decoupling the response.

Theory

Modal Coupling
For this study of modal coupling we shall look at the dynamic properties of a single DOF system. As dynamic descriptors we will use the frequency response and the impulse response which constitute a Fourier transform pair.

$$h(t) \Leftrightarrow H(\omega) \tag{1}$$

Inspecting the impulse response

$$h(t) = 2 \cdot R \cdot e^{-\sigma \cdot t} \sin(\omega_d \cdot t) \tag{2}$$

it is seen that the function can be visualized as a sinusoid at the modal frequency multiplied – or weighted – by an exponential function.

Referring to the convolution theorem [3]: The product of two functions in one domain form the Fourier pair with the convolution of the same functions in the other domain

$$h(t) * f(t) \Leftrightarrow H(\omega) \cdot F(\omega) \tag{3}$$

As shown graphically in Fig. 2, the impulse response may be written

$$h(t) = w(t) \cdot \sin(\omega_d \cdot t) \tag{4}$$

where $w(t) = 2 \cdot R \cdot e^{-\sigma \cdot t}$

Looking at the impulse response as the product of a sinusoid and an exponential decay, the frequency response can be interpreted as a convolution of the decay envelope spectrum

$$W(\omega) = \frac{2R}{\sigma + j\omega} \tag{5}$$

and the sine spectrum

$$X(\omega) = -j \cdot \delta \cdot (\omega - \omega_d) \tag{6}$$

Sustituting in (1)

$$w(t) \cdot \sin(\omega_d \cdot t) \Longleftrightarrow W(\omega) * \delta(\omega - \omega_d) \tag{7}$$

Fig. 2 shows how the impulse response *c*) can be modelled as sinusoid *a*) weighted by an exponential decaying function *b*). The same process in the frequency domain is seen as the sine spectrum *d*), convolved with the spectrum of the exponential decay to yield the frequency response function *f*).

The width of the mode, can be said to be caused by convolution with the decay spectrum.

The frequency response functions in Fig. 2 and subsequent figures show only the magnitude of the positive frequencies of the spectra, and the existence of the negative frequency components as well as the phase spectra should be borne in mind.

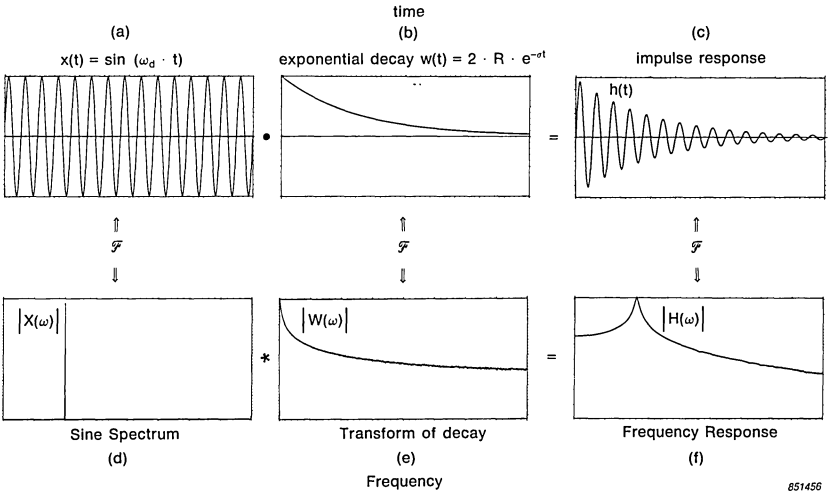

Fig. 2. Illustration of the Convolution Theorem and Fourier Transform pairs

What we can deduce from this exercise is that the line spectrum of the modal frequency is broadened infinitely in the response spectrum, and hence in the frequency response, by convolution with the spectrum of the decay envelope. Since the decay entirely represents the system damping, it may be said that the damping causes the widebanded response.

For systems with multiple DOFs, the impulse response is written as a sum of m single degree of freedom systems, where m is the number of modes in the model

$$h_{ij}(t) = \sum_{r=1}^{m} h_{ijr} = \sum_{r=1}^{m} 2 \cdot R_{ijr} \cdot e^{-\sigma_r \cdot t} \cdot \sin(\omega_{dr} \cdot t) \quad (8)$$

and

$$H_{ij}(\omega) = \sum_{r=1}^{m} W_r(\omega) * \delta(\omega_{dr} - \omega) \quad (9)$$

Again, the smearing effect – or modal coupling – is caused by the convolution with the decay envelope spectrum, except in the case where more than one mode have the same modal frequency.

Deconvolution of the Frequency Response
Having identified the modal coupling to be the result of a convolution with decay envelope spectra, we shall seek a method to deconvolve the response.

First let us perform a mental exercise.

The response signal from an impact excitation shows the same structure as the impulse response. The natural decay may be compensated for by using exponential weighting with a positive exponent

$$w(t) = e^{\sigma_w \cdot t} \quad (10)$$

before the DFT.

The magnitude of σ_w should be the same as the system decay. The resulting signal would be a constant oscillation with the modal frequency(ies) the spectrum of which would be a line(s).

Weighting Function: w(t)							
Hanning T_0 [lines] = 512							
Time constant: τ [lines], ($\sigma = 1/\tau$)							
512	256	125	112	64	32	16	8

T01299GB0

Mathematically this operation can be regarded as a special case of the Laplace transform evaluated close to the pole(s)

$$X(\omega) = \mathcal{F}(x(t) \cdot e^{\sigma_\omega \cdot t}) = \mathcal{L}(x(t)) \Big|_{s = -\sigma_W + j\omega} \quad (11)$$

However this technique is not practically applicable for the following reasons:

1. Since there is always noise present in a practical measurement, this noise will become predominant after a time when the free response has decayed naturally to a level below the noise level, which noise has now been highly amplified by the exponential weighting.

2. Due to the use of a finite transformation, the signal is truncated at some time which results in spectral leakage, giving another convolution which broadens the spectrum.

To consider a more realistic weighting than the "negative decay", the first choice should be the Hanning window because of its excellent sidelobe suppression and ease of implementation [4]. Once again we shall use the single DOF model (2)

$$h(t) = 2 \cdot R \cdot e^{-\sigma \cdot t} \sin(\omega_d \cdot t)$$

Now a multiplication with the Hanning window

$$h(t) \cdot (1 - \cos 2\pi t/T_0) = w_m(t) \cdot \sin(\omega_d) \quad (12)$$

is defined to be the mode response

$$m(t) \equiv h(t) \cdot w(t) \quad (13)$$

where $w_m(t) = 2 \cdot R \cdot e^{-\sigma \cdot t} \cdot (1 - \cos 2\pi t/T_0)$,

and T_0 is the length of the window.

$w_m(t)$ is effectively a much smoother function than $e^{-\sigma \cdot t}$ which can be seen in Fig. 3c.

Using (8) and (9) an extension to multiple DOF systems is made. The Fourier transform of the weighted impulse response

$$\mathcal{F}\left(\sum_{r=1}^{m} w_{mr}(t) \cdot \sin(\omega_{dr} \cdot t)\right) \tag{14}$$

is defined to be the mode spectrum

$$M(\omega) \equiv \sum_{r=1}^{m} W_{mr}(\omega) * \delta(\omega_{dr} - \omega) \tag{15}$$

which has the following properties:

a) Line spectrum structure since $W_m(\omega)$ has a similar frequency distribution to a Hanning spectrum.

b) The bandwidth in the spectrum is determined by the width of the main lobe in $W_m(\omega)$ which itself depends on the weighting function and the DFT transformation size.

c) The peaks are centered over the damped natural – or modal – frequencies independently.

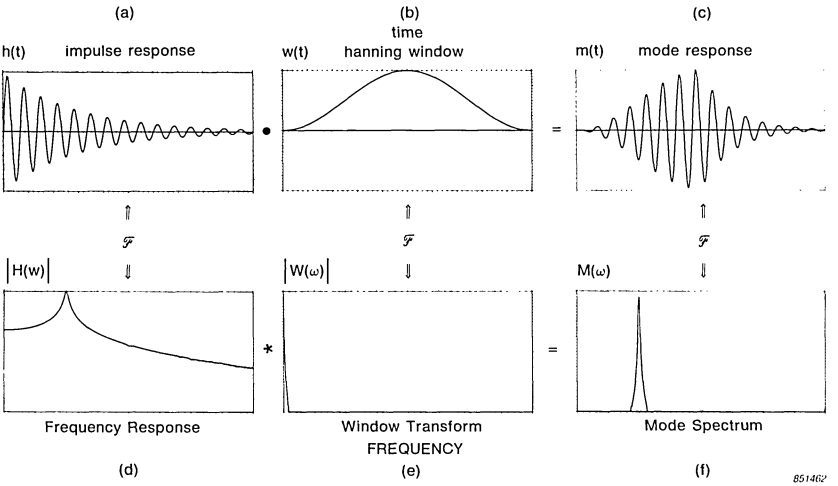

Fig. 3. Illustration of deconvolution of the frequency response by weighting the impulse response

$M(\omega)$ is effectively the frequency response with the damping effect deconvolved.

Fig. 3 illustrates the principles of deconvolution.

If the impulse response *a*) is weighted with the Hanning Window *b*), the resulting "mode response" *c*) is seen to be much smoother. The effect of the same process in the frequency domain shows, that the frequency response *d*) is convolved with the Hanning Spectrum *e*), which has a wider mainlobe but extremely low sidelobes than the decay spectrum of Fig. 2e. The resulting "mode spectrum" *f*) is deconvolved from the damping effect showing only a narrow peak at the damped natural frequency.

Experimental Design
An experiment is designed with the following objectives:

1) To investigate the power of the mode spectrum in determining the number of modes and the associated modal frequencies of a structure with high modal coupling.
2) To determine the properties of the mode spectrum in terms of bandwidth and dynamic range for different weighting parameters.

The experiment is then divided into three sections:

I: The deconvolution of a frequency response synthesized from analytical data. The following table shows the parameters for the synthetic frequency response shown in Fig. 1.

Mode #	Pole		Residue	
	σ [Hz]	ω_d [Hz]	Mag. [m / Ns^{-1}]	Phase [deg.]
1	4	100	10	0
2	4	102	10	180
3	4	200	10	0
4	4	220	1	180
5	4	240	0,1	0
6	8	400	40	180
7	8	410	10	0
8	8	420	1	180
9	8	430	0,1	0
10	30	600	80	180
11	30	610	8	0
12	30	640	0,8	180

T01300GB0

Instrumentation:
Fig. 4 shows the instrumentation. The impulse response is synthesized using a computer, and the data is transferred to a dual channel analyzer for the deconvolution.

II: Synthesis and analysis of weighting functions.

II_a: With a fixed weighting function, the mode spectrum for one mode with alternative decay rates is synthesized.

The data represents the full range from lightly to heavily damped modes.

II_b: With a fixed exponential decay a random noise is added, resulting in a signal-to-noise-ratio of – 6 dB.

Hanning windows with alternative lengths are applied as weighting functions to study the bandwidth and dynamic range in the mode spectrum.

Instrumentation
This experiment is performed analytically using a dual channel analyzer as shown in Fig. 4.

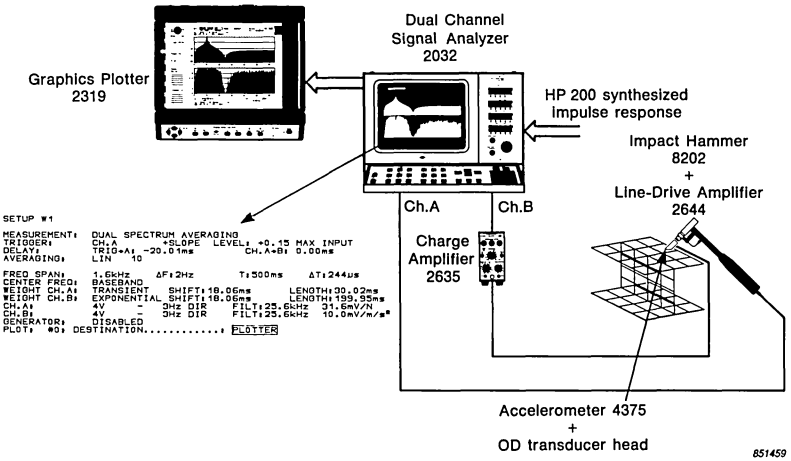

Fig. 4. The instrumentation

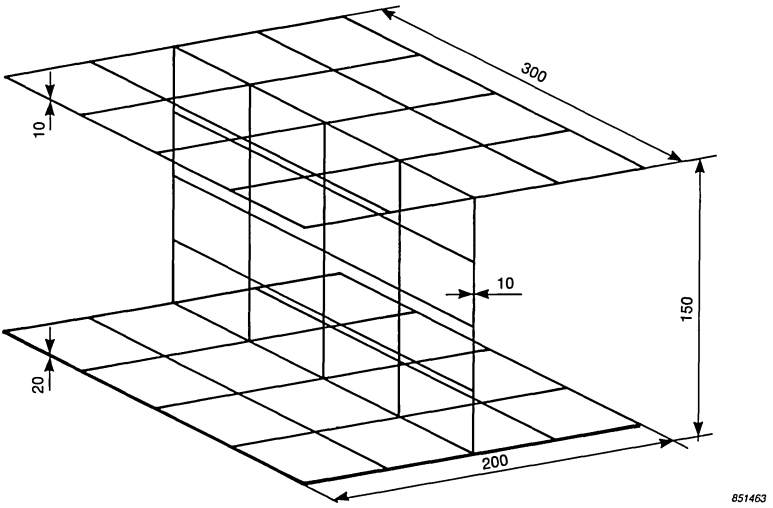

Fig. 5. The structure

III: A measurement of the driving point accelerance is made for an I-beam structure. An oblique DOF is chosen [1] with the purpose of including the maximum number of modes in the experiment.

Structure
The structure is shown in Fig. 5.

Instrumentation:
The instrumentation is shown in Fig. 4.

Excitation
Impact excitation is chosen in order to demonstrate:

a) Deconvolution of the acceleration response spectrum using the acceleration (history) signal.

b) Deconvolution of the frequency response using the impulse response.

Results

Experiment I

Figs. 6 a) and b) show the synthesized frequency response and the associated impulse response. a) also shows a Hanning window in dotted curve of the same width as the full record length. c) shows the impulse response after being Hanning weighted. The transform of c), the mode spectrum d) shows an effective damping decoupling with high mode selectivity.

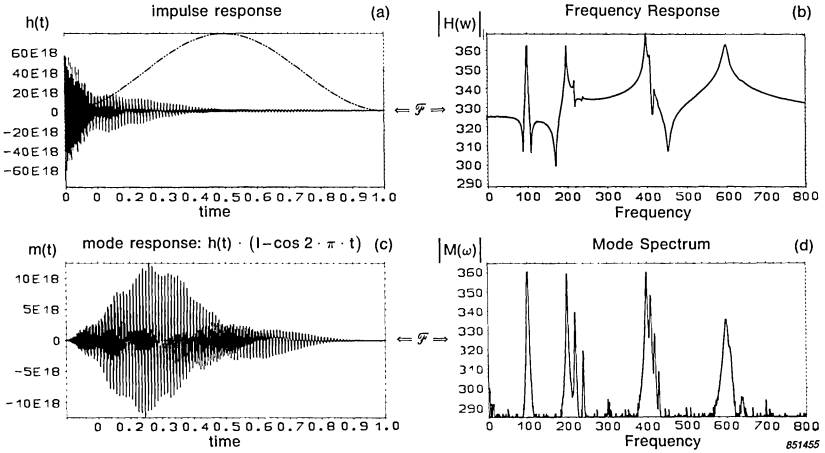

Fig. 6. Experiment I. Deconvolution of the analytical frequency response

Experiment II a

Fig. 7 shows the generated data.

Fig. 7.a shows the decay envelopes due to the modal damping and gives the system time constants.

Fig. 7.c shows each of the decay envelopes weighted with a Hanning window (Fig. 7.b) of equal length to the time record shown. The resulting function are then normalized so that all the results are shown with the same maximum amplitude.

Fig 7.d shows the Fourier transforms of the weighted decays using an arbitrary frequency axes (each centre frequency of the peaks is on an absolute scale 0 Hz).

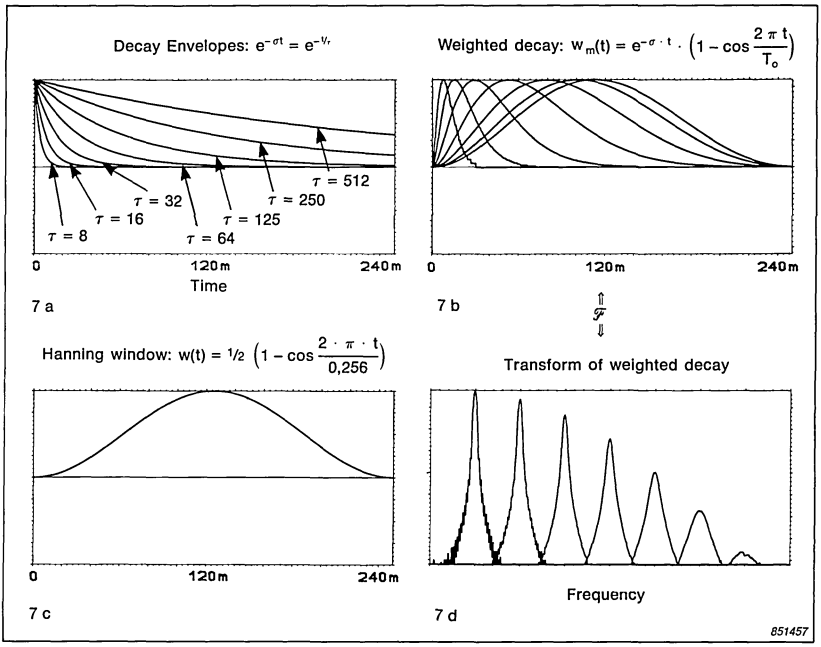

Fig. 7. Experiment IIa. Bandwidth in the mode spectrum for alternative modal dampings

An analysis yields the bandwidth of the peaks in the mode spectra for comparison with the bandwidth of the decay and of the Hanning window. For this analysis the −3 dB bandwidth is chosen. The −3 dB bandwidth for the two functions are:

Hanning [4]: -3 dB Bandwidth $= 1{,}45/T_0$

Exponential: -3 dB Bandwidth $= 2/\tau = 2\sigma$

Table 1 gives a summary of the determination of the ratio of the mode spectrum bandwidth and the system bandwidth. The Hanning bandwidth is fixed 2,9 Hz and the system bandwidth is varied between 0,64 and 40,8 Hz. It is found that the bandwidth in the mode spectrum is equal to or larger than the Hanning bandwidth. With system bandwidths larger than twice the Hanning bandwidth, the peak in the mode spectrum is sharpened to 0,6 of the system bandwidth.

Hanning:								
T_o [s]		0,256						
Bandw./2 [Hz]		2,9						
System:								
τ [s]		0,250	0,125	0,061	0,031	0,016	0,008	0,004
σ = Bandw./2 [Hz]		0,64	1,25	2,61	5,10	10,2	20,4	40,8
Mode Spectrum: Bandw./2 [Hz]		3	3	3,5	4	6	12	25
Mode Spect. Bandw. / System Bandw.		4,7	2,4	1,3	0,8	0,6	0,6	0,6
Remarks		Spect. broadening			Spect. sharpening			

T01301GB0

Table 1. Experiment II a, bandwidth analysis

Experiment II b

Fig. 8.a shows an exponential decay with a time constant of 50 ms and the associated spectrum corresponding to a system bandwidth at 6 Hz. On top of the decay signal a random noise is added resulting in a −6 dB noise/signal ratio.

Figs.8.b to e show the decay weighted with Hanning windows of different lengths and the associated mode spectra.

Table 2 summarizes the effect on the bandwidth and dynamic range of the mode spectrum.

System: Signal/noise		−6 dB			
Bandw./2 [Hz]		3 Hz			
Hanning:	T_o [s]	0,25	0,50	1,00	2,00
Bandw./2	[Hz]	5,8	2,9	1,45	0,73
Dynamic Range	[dB]	~ 60	~ 50	~ 40	~ 25
Mode Speed Bandw. / System Bandw.		2	1,3	0,8	0,6
Remark		Spect. broadening		Spect. Sharpening	

T01302GB0

Table 2. Experiment II b. Synthesized exponential decay measurement with noise. Mode spectrum bandwidth and dynamic range for Hanning windows of different lengths

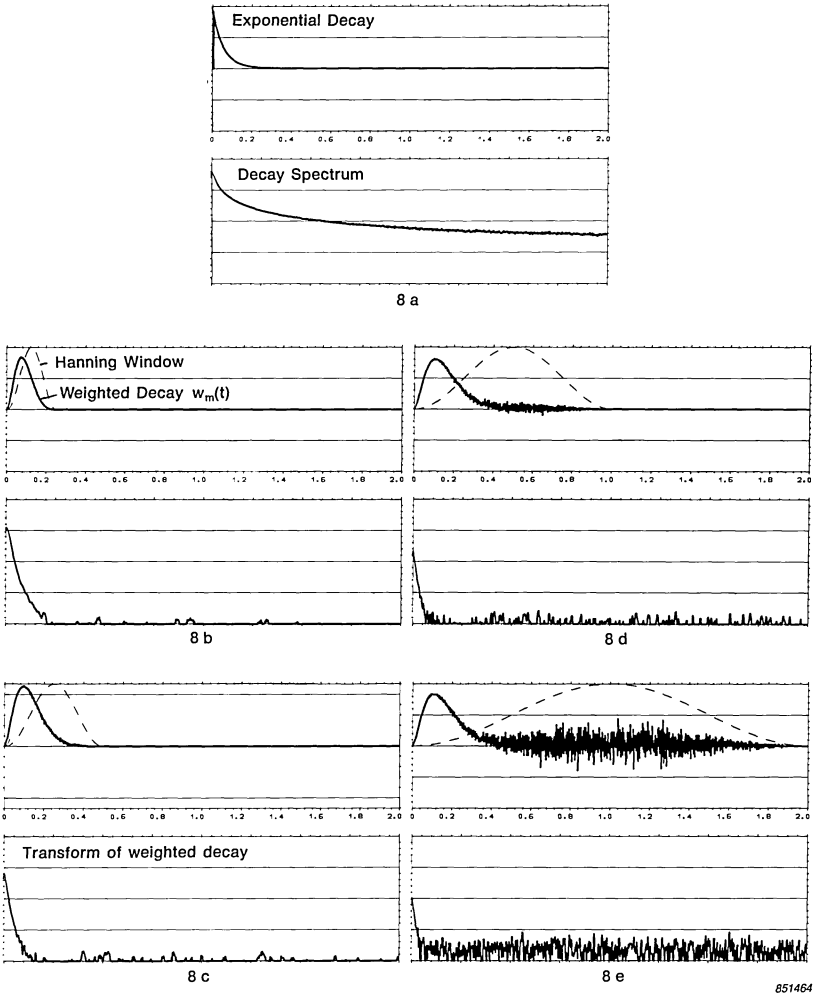

Fig. 8. Experiment IIb. Synthesized exponential decay measurement with noise. Mode spectrum bandwidth and dynamic range for Hanning windows of different lengths

Experiment III
Fig.9 shows the result of a measurement on the I-beam structure.

Two different mode spectra are shown:

1) Deconvolution of the response spectrum by weighting the response to an impact b)

2) Deconvolution of the frequency response by weighting the impulse response estimated from an average from several impacts i).

The associated frequency responses are shown in c) (one impact) and j) (five impacts) respectively. The deconvolved mode spectra are shown in e) and g).

Discussion
The experiments only show results from the use of Hanning windows for the deconvolution of response spectra and frequency responses. However, other windows have been tested during the preliminary experiments, showing the Hanning window to be superior.

Experiment II a indicates, as a rule of thumb:

> For the case where the Hanning bandwidth is larger than the modal bandwidth, that the –3 dB bandwidth in the mode spectrum is equal to the Hanning bandwidth.
>
> For the case where the modal bandwidth is larger than the Hanning bandwidth, that the –3 dB bandwidth in the mode spectrum is equal to 0,6 times the modal bandwidth.

Experiment II_b shows that when noise is present in the response signal or impulse response, the choice of window length is a compromise between bandwidths (mode discrimination) and the dynamic range in the mode spectrum. A recommended choice of window length is one equal to the time constant of the mode or $T_0 = 1/\sigma$. This results in a moderate spectrum broadening, leaving an optimal dynamic range.

Experiment I shows in range a, that it is hard to distinguish modes with modal frequencies spaced closer than half of the mode spectrum bandwidth, and there can only be said to be an improvement with highly damped modes, where spectrum sharpening is obtained.

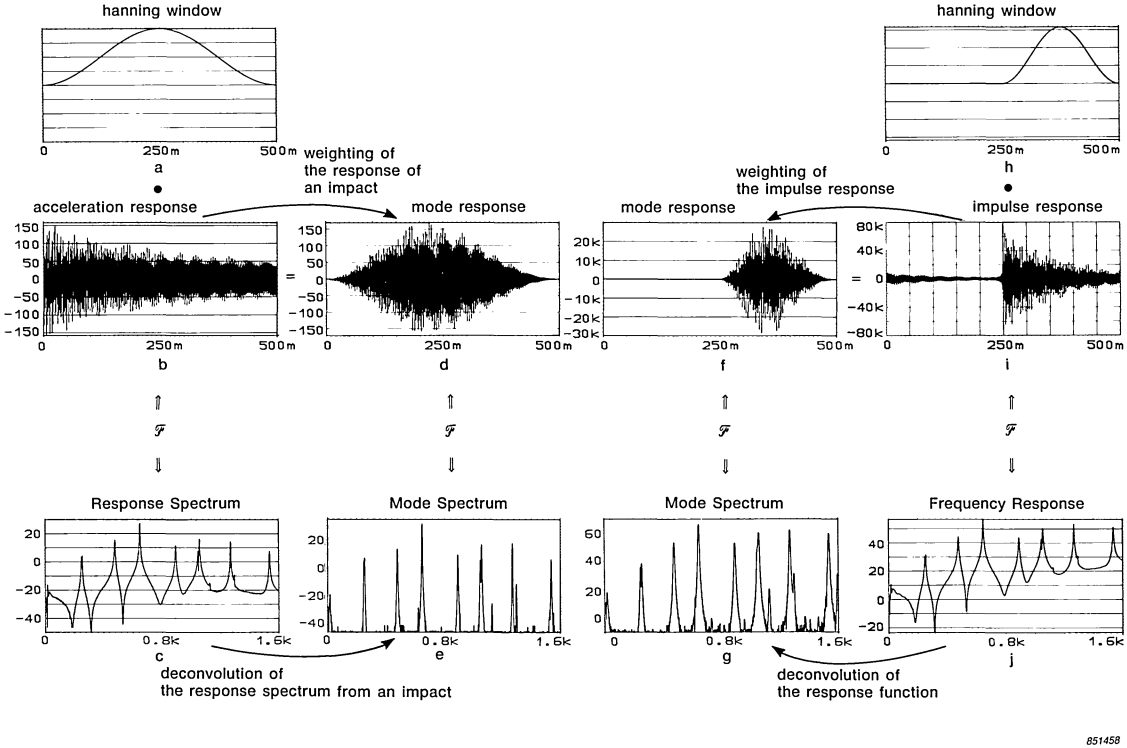

Fig. 9. Experiment III. I-beam measurement. Mode spectra from alternative convolutions

In ranges b and c, closely spaced modes with very large difference in modal strength (up to 60 dB) can clearly be distinguished.

In range d, representing modes with high damping, spectrum sharpening and a very efficient decoupling are observed.

Experiment III demonstrates the effect on real measurements.

The two diverse approaches: weighting of the acceleration response from the impact and weighting of the impulse response, have pros and cons.

In general the acceleration response has a longer duration (more samples) than the impulse response, providing the smallest bandwidth in the mode spectrum. However, this method is inherently applicable with hammer excitation only, and may be contaminated by noise during the measurement.

With shaker excitation, deconvolution is only possible via the impulse response, and this also removes uncorrelated noise in the measurement via the estimation process. However due to the fact that the impulse response only takes up half of the block size in the analysis, T_0 of the window is halved when compared with the acceleration response signal and thus the bandwidth of the mode spectrum is doubled.

In both cases the mode spectrum demonstrates a superior ability to detect the modal frequencies. When comparison is made between the frequency response and the mode spectrum for mode detection using the CRT-display of an analyzer or computer, instead of using a digital plotter as done through this paper, the difference becomes even clearer and favours the mode spectrum.

Conclusion

The experiments show that an efficient decoupling of modes is achieved in the mode spectrum.

The effect is particularly strong when the coupling is caused by large variations in the relative strength between neighbouring modes.

The mode spectrum serves as an excellent detector for identifying modes in a measurement, particularly when the measurement is shown on a CRT display.

Nomenclature

DOF	degree of freedom	$\delta(t)$	delta function = ∞ for $t=0$, 0 for $t \neq 0$
x	response parameter		
f	excitation parameter	$H(\omega)$	frequency response
t	time	$h(t)$	impulse response
$\mathcal{F}$	Fourier tranformation	$\Leftrightarrow\mathcal{F}\Rightarrow$	Fourier transform pair
DFT	discrete Fourier transform	ω_d	modal frequency or damped natural frequency
$\mathcal{L}$	Laplace transformation		
j	imaginary index $=\sqrt{-1}$	σ	decay rate
f	frequency (Hz)	R	modal residue (complex)
ω	frequency (rad s^{-1})	i,j	response and excitation indices
s	Laplace variable (complex)		
$w(t)$	weighting function	r	mode index
T_0	length of weighting window	m	number of modes in model
$W(\omega)$	transform of weighting function	$M(\omega)$	mode spectrum
		$m(t)$	mode response

REFERENCES

[1] DØSSING, O. — "*Improvement of Monoreference Modal Data by Adding an Oblique Degree of Freedom for Reference in Measurements*, IMAC 1986

[2] ALLEMANG, R.J., BROWN, D.L., MERGEAY, M., ZIMMERMAN, R. — "*Parameter Estimation Techniques for Modal Analysis*", SAE Technical Paper Series, no. 790221, 1979

[3] PAPOULIS, A. — "*The Fourier Integral and Its Applications*", McGraw-Hill, 1962

[4] HARRIS, F.J. — "*On the Use of Windows for Harmonic Analysis with the Discrete Fourier Transform*", IEEE Proceedings, Vol.66, no.1, 1978

IMPROVEMENT TO MONOREFERENCE MODAL DATA BY ADDING AN OBLIQUE DEGREE OF FREEDOM FOR THE REFERENCE*

by

Ole Døssing

ABSTRACT

In a modal test the quality of the driving point mobility measurement is rather critical, as it is used for the scaling of dynamic modal model. To ensure that all the modes of interest are excited in this measurement, an oblique asymmetric degree of freedom should be implemented as the reference. This paper describes a transducer head whereby this can be achieved, and results are presented illustrating its advantages over conventional methods.

SOMMAIRE

Dans un test modal, la qualité de la mesure de la mobilité du point d'excitation est assez critique, car celle-ci est utilisée pour l'achèvement du modèle modal dynamique. Pour s'assurer que tous les modes intéressants sont excités lors de la mesure, on doit implémenter comme référence un degré de liberté asymétrique oblique. Cet article décrit une tête de capteur qui le permet, et les résultats sont présentés comme illustration de ses avantages par rapport aux méthodes conventionnelles.

ZUSAMMENFASSUNG

Bei der Modalanalyse ist die Güte der Beweglichkeitsmessung am Erregerpunkt kritisch, da sie zur Maßstabsbestimmung des dynamischen Modal-Modells dient. Um sicherzustellen, daß alle Schwingungsformen angeregt werden, die von Interesse sind, muß ein schiefer, asymmetrischer Freiheitsgrad als Bezug dienen. Dieses läßt sich mit der in diesem Artikel beschriebenen Aufnehmerführung erreichen. Die gezeigten Ergebnisse illustrieren die Vorteile gegenüber konventionellen Methoden.

* First published in IMAC IV, 1986

Introduction

In modal testing using monoreference techniques, that is the measurement of one row or one column of the frequency response function matrix, careful consideration must be given to the choice of the reference degree of freedom (DOF).

The reference, or driving point, measurement must contain all the modes of vibration in the frequency range of interest, and these should ideally be of equal strength.

When the goal of the modal test is to construct a dynamic modal model, the driving point measurement is used in the scaling of the entire model, and hence the measurement quality requirements are critical.

The introduction of an oblique, asymmetric DOF as the reference ensures that all modes appear in the driving point measurement, including those modes whose predominant motion is in only one of the principal directions of the structure.

The implementation of an oblique driving point introduces no theoretical or practical problems with the exception that in general the driving point motion cannot directly be animated.

In this paper a transducer head is presented whereby an oblique DOF can be introduced for the driving point with both ease and precision, and examples are given of the improvements obtained using this as compared to traditional measurement methods.

The experiments prove the efficiency of the technique in terms of more accurate modal parameters. However, when using an attached exciter some rotational inertial loading effect may appear for light structures.

Background and Theory

Monoreference: The Traditional Frequency Response Technique

Experimental modal analysis is mostly based on a data set composed of frequency response functions measured between a set of points/directions (DOFs) spatially distributed over the test structure, and one common reference DOF. Accordingly we shall refer to this as the "monoreference" technique. The term monoreference is introduced to distinguish this technique from others where more than one reference is used.

The monoreference technique is relatively simple, and sufficiently accurate and fast enough for most applications. The boundary conditions for the measurements, that the test object must be excited through only one DOF leaving the rest unconstrained, is also easily achieved.

The ultimate goal of a modal analysis is the creation of the *modal model*, which is not a model of the structure but a model of the dynamics of the structure, valid for specific points/direction (DOF). The number of DOFs needed in order to represent the entire structure depends on the complexity of the structure geometry, and how high a mode shape rank (number) is desired in the analysis.

When DOFs are to be defined for a test structure, they are generally chosen to comply with a coordinate system suitable for the geometric description of the test object – i.e. rectangular, cylindrical, spherical or combinations of these.

As n DOFs have been specified, n × n different input–output combinations exist and hence the same number of different frequency responses are measurable. All of these together form the *frequency response matrix* $[\, H(\omega) \,]$. Each element in $[\, H(\omega) \,] - H_{ij}(\omega)$, represents the response in DOF i per force in DOF j as a function of frequency ω.

For the measurement of this sufficient data set, one DOF is kept fixed for reference – either for response measurement or for the application of excitation. The result is the measurement of one row or one column respectively. As an example, one row is measured in hammer testing where one response transducer is fixed at one DOF and all DOFs are impacted in turn. One column is measured when an exciter is attached to one DOF, and the response transducer is in turn moved to all DOFs.

To extend the discussion, it should be mentioned that in contrast to the monoreference technique other techniques e.g. polyreference exist, where more than one reference is applied, usually in terms of more exciters/columns. The data are in a traditional sense redundant, however application of statistical principles utilizes all the measurements in the estimation of the modal data for improved confidence.

Through this paper we shall only discuss monoreference techniques and the use of the term reference applies equally to response and excitation DOFs.

The Reference
Before choosing the DOF for reference – i.e. which row or column in $[\, H(\omega) \,]$ is to be measured – careful consideration should be given to one or two basic requirements depending on the goal of the measurement:

1. When the objective is to determine the modal frequencies and damping together with the associated mode shapes a first requirement is:

   All modes in the frequency range of interest must be excitable – or have motion at the reference DOF. In other words none of the modes of interest can have a node at the reference DOF.

2. When the objective is to create a mathematical dynamic model representing the structure, then a second requirement also exists:

   A *driving point* measurement, i.e. a measurement with response and excitation both at the reference DOF, must be made for the scaling of the modal data.

The Driving Point Measurement
Bearing in mind that the driving point measurement is the key, and hence determines the accuracy, when representing the modal data in quantitative rather than qualitative terms, the importance of this is now emphasized.

The quality of the driving point measurement is optimised when a DOF is selected where all modes exist in equal strength i.e. the dynamic mass or the scaled modal deflection is of equal magnitude.

In this way the modal coupling [1] effect is minimized. Coupling due to pole location, i.e. close modal frequencies and high damping, is a global property and hence independent of DOF selection.

The Problem

Why it is difficult to obtain accurate Modal Parameters from a Driving Point Measurement
Parameter estimation from the driving point measurement is inherently associated with some difficulties:

1. The modal coupling is at a maximum, since the response at the driving point DOF for all the modes are in phase.

2. Rigid body mode distortion is at a maximum for the same reasons as for 1. Rigid body mode distortion is always found in the most used experimental set-up: soft suspension for simulating a free-free condition. Here six rigid modes exist, three of which are seen in practically any measurement. In accelerance measurements the rigid body distortion shows up as a real constant, equal to one over the combined inertias, added to the measurement. This phenomenon may introduce errors in the parameter estimation (curve fitting) unless some residual terms are added to the model to compensate for it.

In a practical measurement the choice of reference may be aided by a prior knowledge from analytical results or through engineering intuition and a few initial trial measurements.

However, symmetrical structures often exhibit modes with motion which is primarily found along one of the principal geometric axes. This excludes these axes from being good choices for a reference direction. In practice a principal axis is generally the most commonly chosen reference direction. An example on how a principal axis will fail to serve as reference can be illustated by a vertical rigid body mode of a vehicle, where any horizontal plane acts as a node. In this situation, an ideal transducer mounted at a horizontal DOF would detect no motion, and an ideal exciter would not excite this vertical mode.

However real transducers do have some transverse sensitivity responding to the orthogonal motion, just as any practical exciter will introduce some lateral or rotational residual excitation. But the strength of the mode seen from that direction would be weak and the estimation of the associated modal parameters would be contaminated with errors.

The Solution

How an oblique reference DOF reduces the problem
The problems that have been discussed can be significantly reduced if an oblique DOF is introduced for the reference.

For the right combination of position and direction this DOF, inclined to the axes of symmetry, can eliminate the potential problems:

- All modes show motion in **that** particular DOF.
- A balance of the modal strength to give equal magnitude in the frequency response
- One or more of the rigid body modes may be significantly attenuated by allowing the DOF direction to pass through the centre of gyration.

What consequence does the introduction of a DOF which is oblique to the other DOFs have on the Dynamic Model?

First let us make a review of what the dynamic modal model is.

One formulation is the frequency response domain model:

$$\{X(\omega)\} = [H(\omega)]\ \{X(\omega)\} \tag{1}$$

where the frequency response matrix can be written as:

$$[H(\omega)] = \sum_{r=1}^{m} \frac{\{\Phi\}_r \{\Phi\}_r^T}{j\omega - p_r} + \frac{\{\Phi^*\}_r \{\Phi^*\}_r^T}{j\omega - p_r^*} \tag{2}$$

It is directly seen that this model does not include any geometrical parameters in any sense other than the sequence of the DOFs. Hence any direction can be chosen for any point on the structure.

One limitation in the freedom of choice of direction for the DOF is derived from the software used for the documentation – in particular for mode shape plots and animation.

Mode Shape Documentation

How to include an oblique DOF in Animation
One common feature of most software available for modal analysis is that the measured DOFs have to relate to a well defined traditional coordinate system in order to make a graphical presentation of the mode shapes.

This means that an oblique DOF cannot be animated directly. However alternatives can be proposed to circumvent this problem:

1. The simplest solution is simply to omit one single oblique reference DOF from the geometrical model, which can be done without any significant loss of information.

2. Some software products allow the use of local coordinate systems. In these cases the reference DOF can be specified in cylindrical coordinates for inclination with one axes of symmetry, and spherical coordinates when using arbitary inclination.
3. The residues or the mode shapes in the oblique DOF may be decomposed into projections in the global coordinate system, and edited into the modal data set.

Transducer Head Design

How Transducers can be mounted for Oblique Driving Point Measurements

A transducer head has been designed and constructed to aid the precise mounting of response and excitation transducers for oblique reference – and specifically driving point – measurements.

The design criteria were:

- Rugged and compact mounting
- Minimum mass loading
- Minimum stiffness and damping incrementation
- Use with for attached and non-attached exciters
- Unit transmissibility of force and motion from structure to transducers

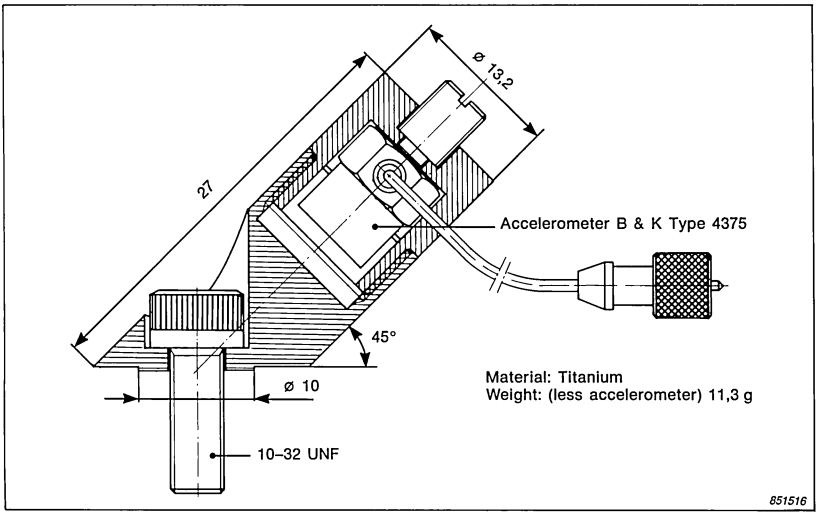

Fig. 1. Transducer head design

Fig. 2. Application of transducer head using an attached exciter

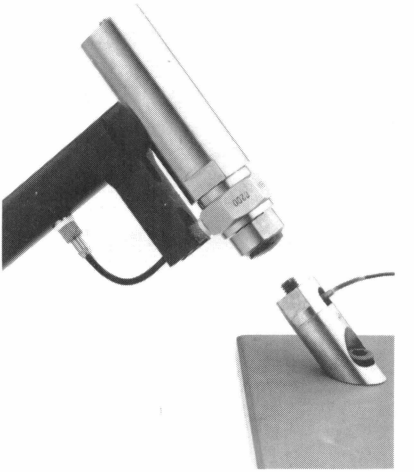

Fig. 3. Application of transducer head using impact excitation

Fig. 1 show the transducer head design. Some of the features are:

- Bolt mounting, where the center line of the transducers cuts the center line of the bolt at the surface of the structure
- Contact surface area is minimised for minimum stiffness and damping modification of the test structure
- Material is Titanium for maximum strength and minimum weight: 11,3 grams
- Accelerometer mounting stud can also serve for force transducer mounting or as an anvil for impact excitation

However, the design is not the result of any prolonged development and is considered to be a prototype for further development.

Figs. 2 and 3 show photographs of the transducer head mounted for shaker - and hammer excitation respectively.

Experimental Design

Two experiments were planned:

I. A test to prove the dynamic characteristics of the transducer head by a ratio calibration [3]. Fig. 7 shows the measurement set up.
II. A test to compare coincident and oblique DOFs for driving point measurements.

Four typical DOFs, one of which was oblique, were chosen, and modal parameters estimated from the measurements.

This second experiment was conducted according to the following plan:

Reference	Excitation	
	Pseudo Random (Shaker)	Impact (Hammer)
Oblique 1	II_a and Reference	II_c
Vertical 2	II_b	II_d

T01304GB0

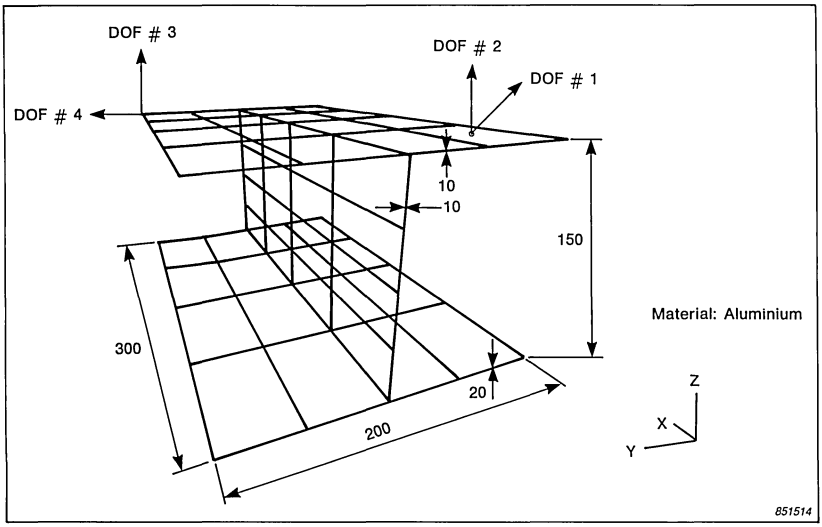

Fig. 4. Test structure with experimental DOFs

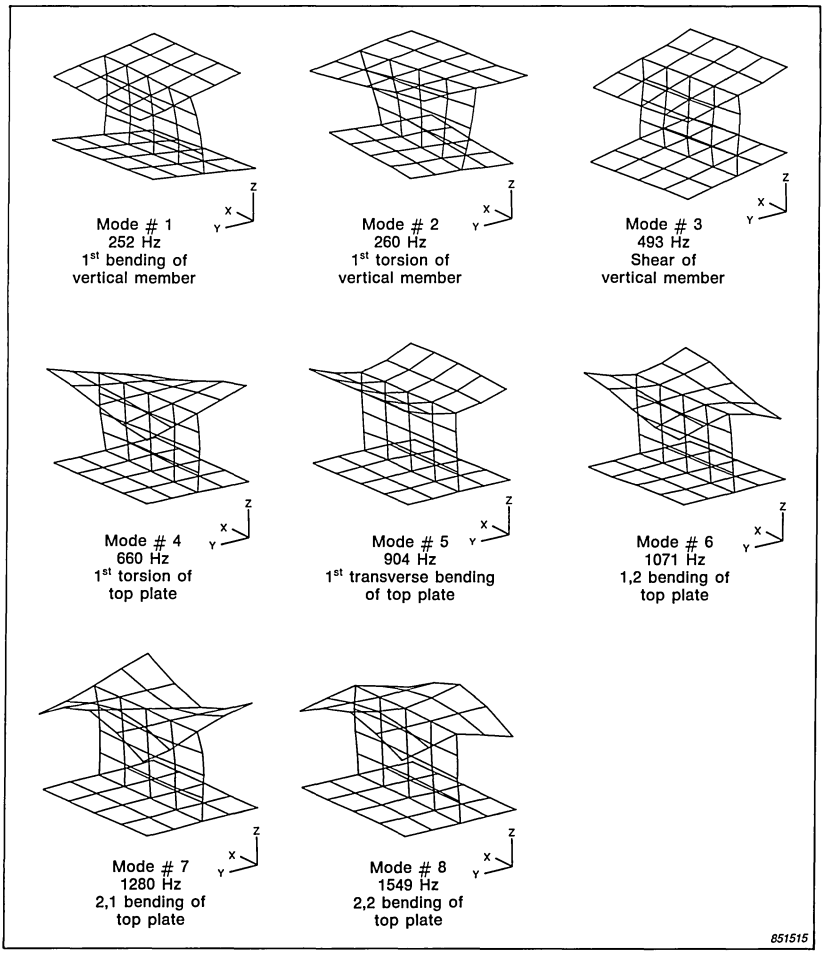

Fig. 5. Mode shapes of test structure

FIXED PARAMETERS

Test Structure: I-beam illustated in Fig. 4. Fig. 5 illustrates the mode shapes for the first 8 elastic modes

Suspension: The structure was placed on rubber foam.

Analyzer Parameters: Frequency Range 0–1600 Hz, 801 lines, Δf = 2 Hz. Other parameters are given in Fig.9 & 11.

Parameter Estimation: Modal 3,0 software by Structural Measurement Systems Inc. Curve fitter: Polynomial [4].

Measured DOF's: Fig. 1. shows 4 typical DOF's selected for the experiment.

Variable Parameters: Excitation: 1) Pseudo Random
2) Impact Hammer

Reference DOF: 1) Oblique no.1
2) Vertical no.2

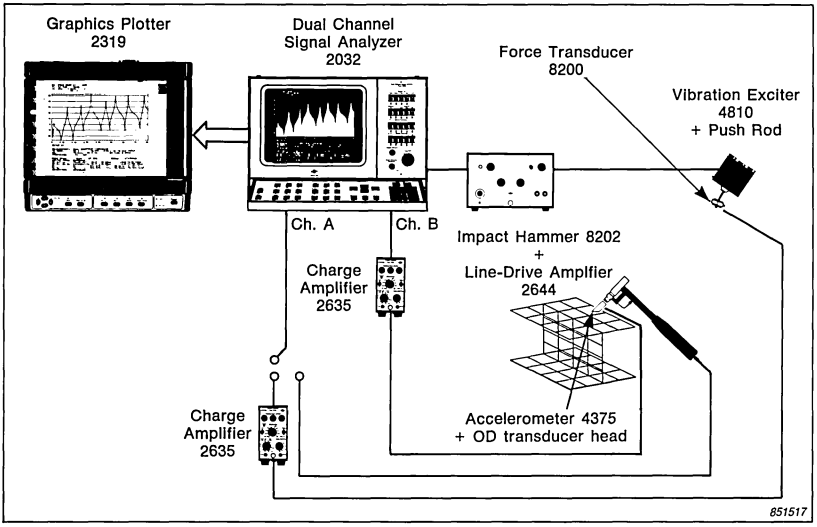

Fig. 6. Instruments used for the experiments

Fig. 7. Checking the dynamic characteristics of the transducer head by mass ratio calibration

Reference Data: For reference, a high resolution measurement was made around mode #1 and #2 in order to gain the highest possible accuracy. Fig. 9 shows a reference driving point measurement together with the analysis parameters.

Measurement Plan

For each of the partial experiments II_a through II_d one column of $[H]$ is measured, using an excitation DOF as reference.

The modal parameters for the two first elastic modes are then estimated by a multiple DOF curve fitter based on a polynomial model [4].

The two first elastic modes are chosen because they illustrate the problems outlined above quite well, as mode #1 manifests predominantly vertical motion for the top plate, and mode #2 manifests predominantly horizontal motion for the top plate (see Fig. 5).

Another feature of modes #1 and #2 are that they are so closely spaced in frequency that they represent a realistic coupling problem.

The frequency range for the experiment was chosen so the first 10 modes were included, representing a minimum practical frequency resolution. However the use of pseudo random noise excitation ensured that leakage errors were not mixed into the experiment.

Results

Experiment I
Fig. 8 shows the dynamic characteristics for the transducer head.

It was found that the frequency response was absolutely flat in the measured frequency range. The sensitivity was equal to that expected: i.e. the nominal sensitivity in the principal axes times the cosine of the angle of inclination.

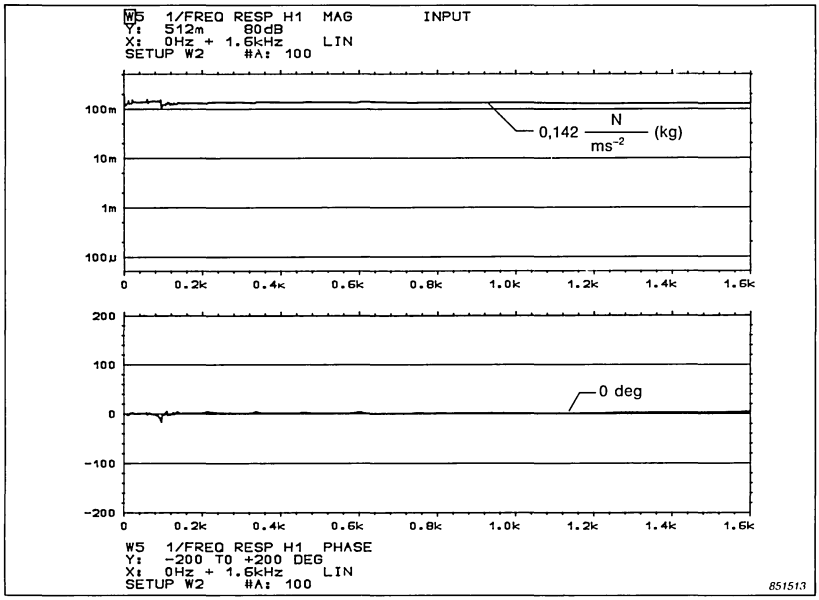

Fig. 8. Frequency response of the transducer head

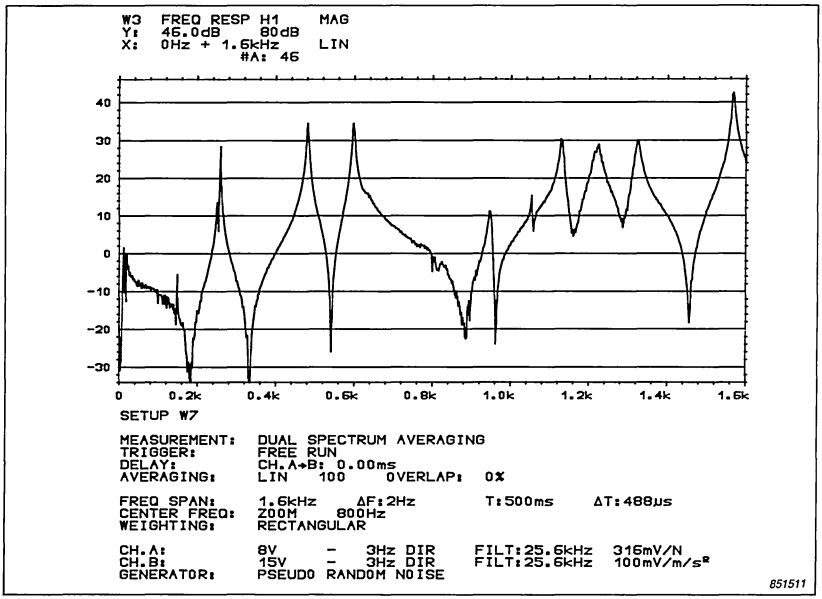

Fig. 9. Frequency response $H_{1,1}$ and analysis parameters Pseudo random excitation

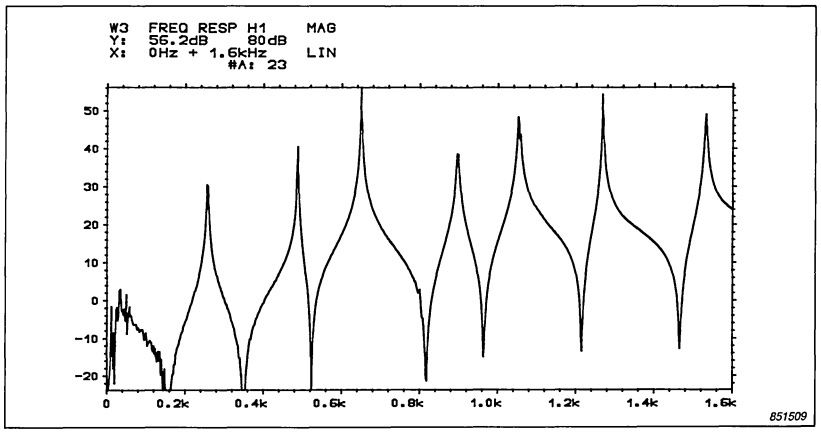

Fig. 10. Frequency response $H_{2,2}$ Pseudo random excitation

The small ripples in the frequency response around 100 Hz were due to some cross resonances in the electro dynamic shaker which could not be

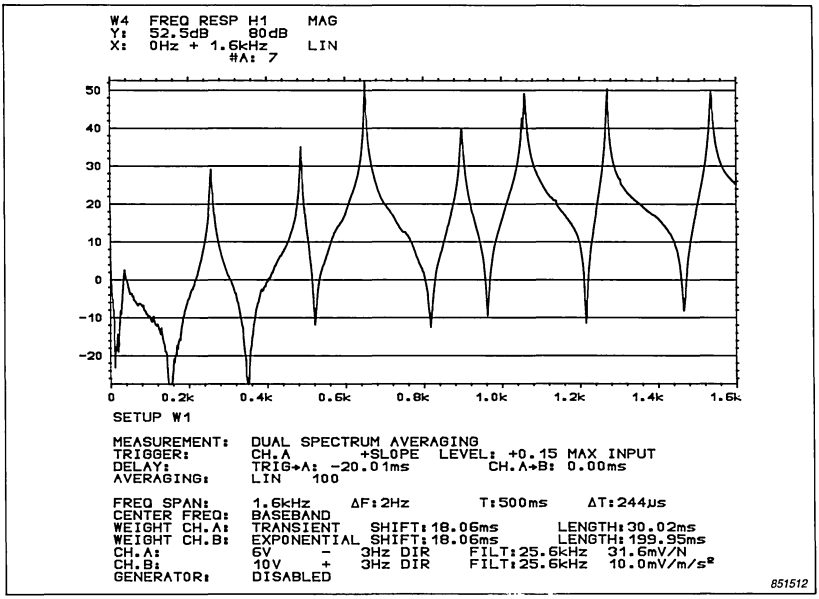

Fig. 11. Frequency response $H_{1,1}$ Hammer excitation

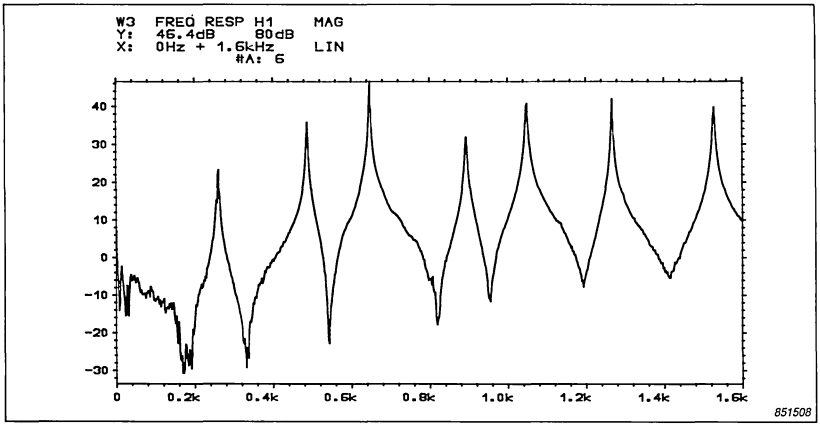

Fig. 12. Frequency response $H_{2,2}$ and measurement parameters Hammer excitation

removed in the frequency response estimation procedure since this "noise" is coherent with the desired excitation.

Experiment II

Figs. 9 through 11 show the driving point frequency response for the four partial experiments as well as for the reference measurement.

Table 1 presents an extract of the estimated modal parameters, in terms of the modal frequency and the magnitude of the residues, for the two first elastic modes for the four DOFs in the measurements.

Table 2 shows the partial shape of the first two modes. The mode shapes are scaled to unit modal mass [2].

Modal Deflections (Unit Modal Mass) (Magnitude)			
Experiment II_a		Experiment II_c	
Mode 1	Mode 2	Mode 1	Mode 2
0,595	1,222	0,771	1,205
2,067	0,133	1,587	0,281
1,928°	2,253	2,365	1,558
0,704	2,324	0,178	2,050
(normal)	(normal)	(normal)	(normal)
Experiment II_b		Experiment II_d	
Mode 1	Mode 2	Mode 1	Mode 2
0,797	0,238	1,026	0,744
2,005	0,483	1,967	0,646
1,924	0,137	2,649	1,370
0,535	0,278	0,007	2,050
(normal)	(complex)	(normal)	(complex)
Pseudo Random		Hammer	
Reference			
Mode 1	Mode 2		
0,595	1,220		
2,067	0,118		
1,928	2,177		
0,704	2,385		
(normal)	(normal)		

T00926GB0

T00927GB0

Table 1. Modal Parameters for modes #1 & #2 using different measurement techniques. The driving point measurements are given in bold

Accelerance Residues (Magnitude) and Modal Frequencies			
Experiment II_a		Experiment II_c	
Mode 1 (251,8 Hz)	Mode 2 (259,3 Hz)	Mode 1 (257,4 Hz)	Mode 2 (260,9 Hz)
51,5	**249,2**	**98,1**	**242,8**
192,8	27,1	201,8	56,6
175,3	458,5	300,9	313,9
64,3	472,8	22,7	229,0
Experiment II_b		Experiment II_d	
Mode 1 (257,1 Hz)	Mode 2 (260,1 Hz)	Mode 1 (257,7 Hz)	Mode 2 (261,3 Hz
263,1	19,1	333,1	80,4
662,1	**38,9**	**638,6**	**69,8**
635,3	11,0	860,2	148,1
176,7	22,3	22,7	221,6
Pseudo Random		Hammer	
Reference			
Mode 1 (251,7 Hz)	Mode 2 (259,2 Hz)		
57,1	**247,0**		
198,3	22,6		
185,0	440,1		
67,5	483,0		

T00929GB0

T00928GB0

Table 2. Partial shapes of mode #1 & #2 using different measurement techniques. The descriptor "normal" is assigned to the shapes where all DOFs have a phase relation within ± 5°

Discussion

Transducer Head Dynamics

From experiment I, the mass ratio calibration shows that the transducer head serves its main purpose – to transmit force and motion without "colouring" the measurements. However, experiment II showed that mounting the force transducer at the top of the transducer head introduces rotational inertia loading of the structure which has to be very carefully considered when testing light structures.

Oblique versus Vertical Driving Point Measurements

Comparing the measured $H_{1,1}$ (Figs. 9 and 11) with $H_{2,2}$ (Figs. 10 and 12) it appears that mode #2 – predominantly horizontal motion – cannot be

observed by the naked eye in a vertical driving point measurement as the modes are closely spaced.

From Table 1 it is seen that the difference in magnitude of the residues is large for vertical driving point measurements thereby increasing the modal coupling. Comparing the partial mode shapes in Table 2 it is seen that mode shape #2 is very poorly estimated from measurements made with a vertical driving point.

Structural Loading from the Transducer Head

When comparing $H_{1,1}$ measured with attached and non-attached exciters respectively (Figs. 9 and 12) a surprising discrepancy appears. In particular, for frequencies above 800 Hz it is seen that the modal frequencies are shifted significantly down in frequencies.

This phenomenon is identified to be the effect caused by rotational inertia loading added to the system by the mounting of the force transducer (21 grams) and cables on top (20 mm above surface) of the transducer head. As can be seen from the mode shape plots (Fig. 5) the

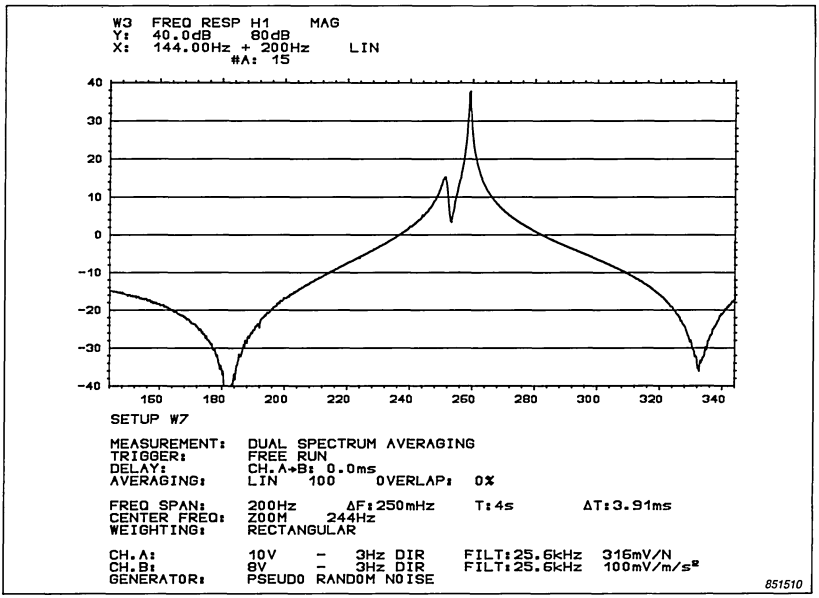

Fig. 13. Frequency Response $H_{1,1}$ and analysis parameters for high resolution reference measurement. Pseudo random excitation

higher modes show the largest rotations of the top plate, and hence the highest sensitivity for rotational inertia loading.

However the test structure is very light and the loading problem will probably not exist for most practical structures.

The loading effect is significantly reduced when the force transducer is mounted beneath the transducer head. Assuming that oblique force is equal to its vertical projection, the sensitivity can be corrected.

Conclusion

The experiments show that the use of an oblique DOF for reference, in particular for driving point measurements, improves the quality of the estimated modal parameters.

When modes closely spaced in frequency show predominantly orthogonal motion, the oblique reference exhibits a strong decoupling effect.

Use of a non-attached exciter (hammer) does not introduce any inertia loading effect on the structure.

Attached versus Non-Attached Exciter

Due to the discovery of the loading effect from the force transducer, a quantitative comparison cannot be made between the modal parameters found from the two alternative measurement techniques. However, subjective evaluation suggests that the discussion concerning oblique v.s. vertical reference is equally valid for both methods.

The transducer head design for making oblique driving point measurements shows good frequency characteristics. However when used on structures with large rotations at the mounting point, an inertia loading effect is observed.

Nomenclature

$\{ X(\omega) \}$	response vector. Elements representing the response spectrum in each DOF
$\{ F(\omega) \}$	excitation vector. Elements representing the force spectrum in each DOF
DOF	degree of freedom (point & direction)
$[H(\omega)]$	frequency response matrix
$H_{ij}(\omega)$	frequency response function

p	pole location (complex) $p = -\sigma + j\omega_d$
ω_d	modal frequency (damped natural frequency)
σ	decay rate
R	residue (complex)
m	number of modes in model
r	mode index
i, j	response DOF and excitation DOF indices
$\{\Phi\}$	mode shape (vector of modal displacements)
j	imaginary index $j = \sqrt{-1}$

References

[1] DØSSING, O. — "*A Method of Determining the Modal Frequencies of Structures With Coupled Modes*", IMAC 1986.

[2] BROWN, D., CARBON, G., RAMSEY, K. — "*Survey of Excitation Techniques Applicable to the Testing of Automotive Structures*", SAE Technical Paper Series, no. 77029.

[3] ALLEMANG, R.J., BROWN, D.L., MERGEAY, M., ZIMMERMAN, R. — "*Parameter Estimation Techniques for Modal Analysis*", SAE Technical Paper Series, no. 790221, 1979.

[4] RICHARDSON, M.H., FORMENTI, D.L. — "*Parameter Estimation from Frequency Response Mesurements using Rational Fraction Polynomials*", Proceedings of the 1st International Modal Analysis Conference 1982.

News from the Factory

Sine/Noise Generator Type 1049 and
Sine Generator Type 1051

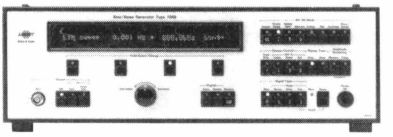

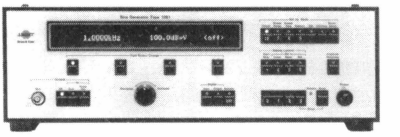

The Sine/Noise Generator Type 1049 and Sine Generator Type 1051 are microprocessor-based, ATE type instruments which integrate the needs of high signal purity and accuracy with ease of use and extreme versatility.

The Generators are equipped with linear and logarithmic sweep ranges, each with their own frequency limits which can be preset by the user from 0,2 Hz to 200 kHz. Extended linear frequency sweeps from 0,001 Hz to 200 kHz may also be obtained with frequency resolution of 1 mHz. Single and repetitive sweep modes, plus accurate four-digit sweep rate selection, permit operation with graphic recording and oscilloscope monitoring equipment. Output levels from 100 μ V to 5 V RMS are selectable with attenuator accuracy of 0,03 dB and amplitude which is flat within 0,05 dB in the audio range. Output distortion is guaranteed better than –96 dB in the audio range and is typically –110 dB down at a frequency of 1 kHz.

The powerful, easy-to-use IEEE interface of the generators makes them easy to be integrated rapidly in one's automatic test system. Following the simple software instructions *all* front panel functions can be set up as well as a number of system checks can be performed via the interface. For stand-alone use, a logically laid-out control panel and 40-character alphanumeric display enable one to set up the generators quickly and accurately. Single test frequencies or pre-programmed sweeps can be output with a few simple keystrokes. During tests the display continually updates, showing instantaneously the frequency and level. For frequently repeated tests, nine complete sets of control panel settings can be stored so that they are readily available when needed.

For added versatility, the 1049 Generator has a number of extra facilities. These include narrow-band random, white and pink noise outputs for electroacoustic measurements, a logarithmic amplitude sweep for establishing clipping and distortion limits of electronic circuits, and a compressor providing a 126 dB of "live" amplitude regulation to maintain a constant output level with sound and vibration excitation equipment. Furthermore, the compressor provides a convenient means of teaching the 1049 a memory-weighted frequency sweep from a measured response signal.

Vibration Exciter Control Type 1050

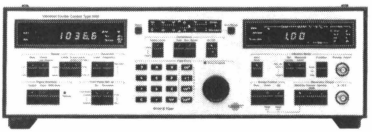

The Vibration Exciter Control Type 1050 is a digital instrument for use as a sinusoidal sweep controller of electrodynamic vibration exciter systems. The IEEE interface and frequency generation resolution to 1,19 mHz makes the Type 1050 a flexible and highly accurate instrument. It forms the basis of an analyzing system which has specific application to engineering development and prototype testing; quality control; resonance dwell testing and vibration transducer calibration.

Piezoelectric accelerometers and force transducers can be directly connected to the Type 1050 for control of any vibration measurement parameter, or for vibration measurement.

Complex test programmes, using up to nine different vibration levels, can be preset and stored in non-volatile memories. Constant levels of force, acceleration, velocity and displacement can be attained using the compressor, which has a dynamic range of 100 dB. These features permit complex tests conforming to national and international standards to be easily performed.

The Type 1050 is simple to operate with a field entry keyboard and thumbwheel as well as a sequence to guide the user through the test set-up parameters in a logical order. Complete system control is possible using a desk-top calculator, and easy data transfer and documentation can be achieved via the IEEE digital interface.

PREVIOUSLY ISSUED NUMBERS OF BRÜEL & KJÆR TECHNICAL REVIEW

(Continued from cover page 2)

4-1980 Selection and Use of Microphones for Engine and Aircraft Noise Measurements.
3-1980 Power Based Measurements of Sound Insulation.
Acoustical Measurement of Auditory Tube Opening.
2-1980 Zoom-FFT.
1-1980 Luminance Contrast Measurement.
4-1979 Prepolarized Condenser Microphones for Measurement Purposes.
Impulse Analysis using a Real-Time Digital Filter Analyzer.
3-1979 The Rationale of Dynamic Balancing by Vibration Measurements.
Interfacing Level Recorder Type 2306 to a Digital Computer.
2-1979 Acoustic Emission.
1-1979 The Discrete Fourier Transform and FFT Analyzers.
4-1978 Reverberation Process at Low Frequencies.
3-1978 The Enigma of Sound Power Measurements at Low Frequencies.
2-1978 The Application of the Narrow Band Spectrum Analyzer Type 2031 to the Analysis of Transient and Cyclic Phenomena.
Measurement of Effective Bandwidth of Filters.
1-1978 Digital Filters and FFT Technique in Real-time Analysis.

SPECIAL TECHNICAL LITERATURE

Brüel & Kjær publishes a variety of technical literature which can be obtained from your local B & K representative.
The following literature is presently available:

- Mechanical Vibration and Shock Measurements (English), 2nd edition
- Modal Analysis of Large Structures–Multiple Exciter Systems (English)
- Acoustic Noise Measurements (English), 3rd edition
- Architectural Acoustics (English)
- Strain Measurements (English, German)
- Frequency Analysis (English)
- Electroacoustic Measurements (English, German, French, Spanish)
- Catalogues (several languages)
- Product Data Sheets (English, German, French, Russian)

Furthermore, back copies of the Technical Review can be supplied as shown in the list above. Older issues may be obtained provided they are still in stock.

Printed in Denmark by Nærum Offset

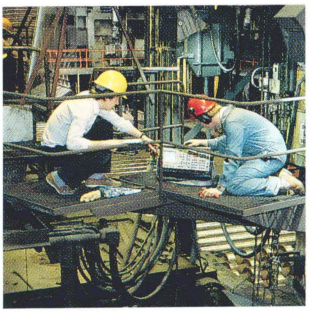

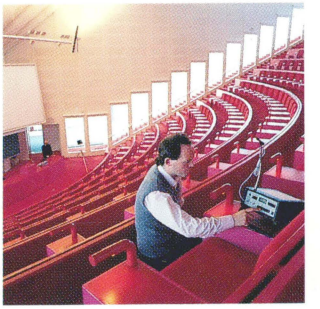

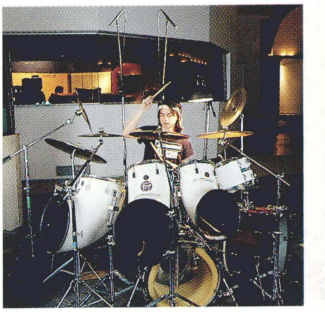

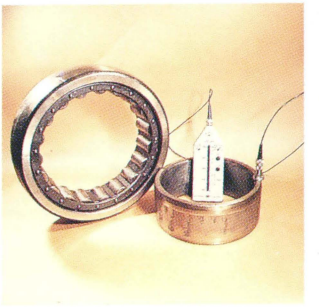

BV 0026-11

Brüel & Kjær

DK-2850 NÆRUM, DENMARK · Telephone: + 45 2 80 05 00 · Telex: 37316 bruka dk